Received: 11 November 2022 | Revised: 24 January 2023 | Accepted: 25 February 2023

DOI: 10.1002/jrs.6514

SPECIAL ISSUE - RESEARCH ARTICLE

Journal of RAMAN SPECTROSCOPY WILEY

Using Raman spectroscopy to detect scytonemin of epiliths and endoliths from marble, serpentinite and gypsum

Jan Jehlička[1] | **Adam Culka**[1] | **Kateřina Němečková**[1] | **Jan Mareš**[2,3]

[1]Institute of Geochemistry, Mineralogy and Mineral Resources, Faculty of Science, Charles University, Prague, Czech Republic

[2]Biology Centre of the Czech Academy of Sciences, Institute of Hydrobiology, České Budějovice, Czech Republic

[3]Center Algatech, Institute of Microbiology, The Czech Academy of Sciences, Třeboň, Czech Republic

Correspondence
Jan Jehlička, Institute of Geochemistry, Mineralogy and Mineral Resources, Faculty of Science, Charles University, Prague 12843, Czech Republic.
Email: jehlicka@natur.cuni.cz

Funding information
Czech Science Foundation, Grant/Award Number: 21-03322S; Center for Geosphere Dynamics, Grant/Award Number: UNCE/SCI/006

Abstract

Here, we present Raman spectra showing the presence and distribution of scytonemin and carotenoids in epilithic and endolithic colonisations from temperate locations in Central Europe and Sicily. In the Bohemian Massif, marble and serpentinitic cyanobacterial epiliths dominated by cyanobacteria *Scytonema*, *Stigonema*, *Hassallia*, *Gloeocapsopsis* and *Gloeocapsa* were investigated using light microscopy and Raman spectroscopy. Scytonemin was a common dark pigment, accompanied by carotenoids and gloeocapsin on the marbles from Opolenec and on serpentinites from Holubov (South Bohemia). Raman spectra from other sites originated from endolithic colonisations of gypsum. They were located in the Carpathian foredeep (Badenian, Silesian unit, eastern Poland) and in Messinian complexes in the Mediterranean area (Sicily). Similarly to the previous localities, almost ubiquitous occurrence of scytonemin confirmed the presence of cyanobacterial colonisations. Obtained findings are important from the spectroscopic point of view. Additionally, comparing results from several sites confirmed the common occurrence of scytonemin in both endoliths and epiliths from areas that cannot be considered climatically extreme, although they experience rapid fluctuations in temperature, humidity and UV irradiation on the exposed rocky substrates.

KEYWORDS

cyanobacteria, endolithic colonisations, epilithic colonisations, Raman spectra, scytonemin

1 | INTRODUCTION

As Walker and Pace stated in their excellent review, 'The endolithic environment, the pore space within rocks, is a ubiquitous habitat for microorganisms and a critical interface between biology and geology'.[1] Sometimes, microbes thrive and colonise mineral or rocky outcrops.[2,3] They sometimes colonise surface, cracks or cleavage spaces of gypsum,[4,5] calcite,[6] dolomite[7] or granite.[8,9] These organisms are known as lithobionts and can be divided into several groups—epiliths (inhabiting the surface of rocks), endoliths (inhabiting inner parts of rocks) and hypoliths (inhabiting spaces below rocks).[10] Endoliths can be further divided into chasmoendoliths (colonising rock fissures and cracks) and cryptoendoliths (colonising pores within rocks).[2] These lithobionts include diverse groups of organisms—microalgae, lichens, fungi, cyanobacteria and archaea.[11,12]

Marble and granite are the most common rocks covered by black, dark or reddish microbial, frequently cyanobacterial colonies.[13] Rock surfaces can be fully exposed to sunlight and occur also in all types of tropical biomes, including the table mountains in the Guayana Uplands of South America[14] inselbergs (isolated rock outcrops) in rainforests, humid and dry savannas[15] and semideserts.[16] These rock surfaces harbour a surprisingly high variety of cyanobacteria and cyanobacterial lichens thriving in the harsh environments.[16]

Colourful patches on rocky outcrops, building stones, statues or on surface of trees have sometimes origin in microbial colonisation.[17–20] Microbial world is colourful, and the pigmentation reflects different possible functions of the synthesised pigments. Not all are used for photosynthesis (chlorophylls, carotenoids), and some of them participate in processes allowing microbes to protect themselves against environmental stressors such as UV radiation, for example, mycosporine-like amino acids and scytonemin.[21] Orange, pink, reddish and yellow carotenoids are widespread not only among photosynthetic prokaryotes.[22,23] Many other classes of pigments are encountered in the microbial world: Examples include chlorophylls and bacteriochlorophylls; phycobiliproteins; retinal-containing proteins such as bacteriorhodopsin, halorhodopsin and proteorhodopsin; carotenoids; flexirubins; and many others.[24,25] Phototrophic prokaryotes can also display brown, violet and blue colours as reflected in names such as *Chlorobium phaeovibrioides*, *Rhodocyclus purpureus* and *Cyanothece aeruginosa*. Properties such as the colony colour and the presence of different pigments are useful for taxonomic characterisation of prokaryotes,[22] and the pigments may even be used as biosignatures for search of life in astrobiology.[26,27] The chemical structure of some microbial pigments is still unknown, such as the pigment of the marine proteobacterium *Phaeobacter inhibens*,[28] gloeocapsin found in several cyanobacteria[29,30] or glaukothalin of *Rheinheimera baltica*.[31]

Scytonemin is a very common protective pigment of cyanobacteria, exclusively produced by this group of microorganisms, thus serving as a specific biomarker.[32–35] It was documented by Raman spectroscopy in various samples, for example, by endolithic cyanobacteria from the Atacama Desert[36–39] or from cold zones.[40,41] Scytonemin has the following formula: $C_{36}H_{20}N_2O_4$. A yellow-brown lipid-soluble dimeric compound is composed of indolic and phenolic subunits,[42] and it occurs in oxidised (MW 544 Da) and reduced (MW 546 Da) forms.[43]

The application of Raman spectroscopy (resonance Raman spectroscopy) in natural pigments research, mainly to study carotenoids and chlorophylls, has developed since 1980s.[44] The technique was also used to assess the presence of light-harvesting pigments bacteriochlorophyll and bacteriochlorophyll-protein complexes in purple photosynthetic bacteria.[45] Resonance Raman spectra of astaxanthin-protein complexes were published soon after, allowing to deepen the knowledge of carotenoid-protein interactions.[46] More achievements of the technique appeared later on photosynthetic and protective pigments of very different microorganisms, including extremophillic ones, as reviewed, for example, by Jehlička et al. and Maia et al.[47,48] Raman spectroscopy was suggested as an excellent tool to rapidly prospect, detect and discriminate pigments on rocky outcrops.[49,50]

Scytonemin was reported from rocky colonisations of different types many times as detected using Fourier transform (FT)-Raman spectroscopy with 1064-nm excitation. These studies describe colonisations from different cold areas, for instance,[51,52] or from warm desert zones, more commonly using 785 nm[53] but also using FT-Raman spectroscopy with 1064-nm excitation.[54] The spatial distribution of scytonemin and other pigments was evidenced using different techniques of Raman spectroscopic mapping or imaging. This information is more and better reported mainly from endoliths in different lithologies from the Atacama Desert (e.g., Vítek et al., 2013).[4]

The first Raman spectroscopic analysis of scytonemin was reported from the purified extracted material obtained from *Lyngbya* cf. *aestuarii* from intertidal cyanobacterial mats by Edwards et al.[55] The measurements were carried out using an FT-Raman with 1064-nm Nd:YAG excitation. The authors described the key spectroscopic signatures and suggested for the first time assignments of all Raman bands. The Raman spectrum of scytonemin includes four major diagnostic Raman bands at 1590, 1549, 1323 and 1172 cm^{-1}. The tentative assignments of the most important scytonemin bands are as follows: The 1590 cm^{-1} band is assigned to the ν(CCH) aromatic ring quadrant stretching vibration, the 1549 cm^{-1} band is assigned to the ν(CCH) *p*-disubstituted aromatic ring vibration, the 1323 cm^{-1} band is attributed to the ν(C=N) stretching vibration of the indole ring and the 1172 cm^{-1} band arises from the ν(C=C–C=C) system (*trans*) that can be followed throughout the molecule and is possibly centred on the important ν(C–C) vibration of the dimer bond between the two parts of the molecule.

Raman signatures of carotenoids from different sites with less extreme environmental conditions (compared with the deserts and polar regions) were already reported[5,56] from gypsum endoliths from Sicily. Some data were collected directly in the field at gypsum outcrops using portable Raman spectrometer.[57] They are also common photosynthetic pigments connected to the

cyanobacterial endolithic colonisations at different sites in eastern Poland as reported recently.[50]

In this study, we focus on the dark protective pigment scytonemin from rocks from three different, climatically temperate areas. Investigated outcrops include gypsum endoliths and marble and serpentinite epiliths from Central European and Sicilian sites. The Raman measurements are accompanied by optical microscopic analysis of detected microbial communities. Our aim was to show that the spectroscopic data and detected pigments can be associated with the presence of the identified cyanobacteria.

2 | MATERIALS AND METHODS

2.1 | Sampling sites

Investigated sites of colonised marble and serpentinite occurrences studied belong to Bohemian Massif (Czechia), and outcropping gypsum is of Badenian age (eastern Poland) and those Messinian age (Sicily). Figure 1 reports a simplified map with the positions of the localities, and Table 1 lists the sampling sites.

2.1.1 | Opolenec

Samples of epiliths were collected in the Opolenec Nature Reserve, on steep west-oriented slopes of the Opolenec hill in Šumavské Podhůří mountain range (forest-steppe pine wood), close to the town of Vimperk, South Bohemia, Czechia. The rocks belong to Bohemian Massif (Moldanubicum) and consist of a metamorphosed limestone lens embedded in gneisses. Two sampling spots included crystalline limestone (marble) outcrops exposed to direct sunlight in the area of a small karst cavern (Sudslavická Cave; GPS: 49.0905586° N, 13.7958778° E (Figure 2A) and an abandoned historical quarry nearby.

2.1.2 | Holubov

The second sampling site in South Bohemia included two sub-localites, the Holubovké hadce Nature Reserve (GPS: 48.8924278° N, 14.3423711° E) and another spot outside the Bořinka Nature Reserve (GPS: 48.9001161° N, 14.3094308° E), both near Křemže, in the Blanský les Protected Landcape Area. Both localities are also part of the Bohemian Massif (Moldanubicum) and contain serpentinite outcrops on hillslopes of the Křemžský Brook, covered by a sparse pine wood. The samples of epiliths were taken from sunlit serpentinite outcrops in the Holubovské hadce site (Figure 2C).

FIGURE 1 Map of the site with investigated epilithic and endolithic occurrences.

2.1.3 | Skorocice

Gypsum samples were collected from weathered areas of the gypsum outcrop close to the village Skorocice (GPS: 50.4181372° N, 20.6706975° E). Colonisation was green and blackish coloured and were located mostly in the cleavage zones of flat honey colour gypsum crystals (around 10 cm in length). The blackish colonisation was located always in the areas closer to the surface.

TABLE 1 List of sampling sites.

Country	Locality (*site*)	GPS coordinates	Lithology	Type of colonisation
Czechia	Opolenec *(Opolenec Nature Reserve)*	49.0905586° N, 13.7958778° E	Marble	Epiliths
	Holubov *(Holubovké hadce Nature Reserve)*	48.8924278° N, 14.3423711° E	Serpentinite	Epiliths
	Holubov *(Bořinka Nature Reserve)*	48.9001161° N, 14.3094308° E	Serpentinite	Epiliths
Poland	Skorocice	50.4181372° N, 20.6706975° E	Gypsum	Endoliths
	Chotel Czerwony	50.3715161° N, 20.7284994° E	Gypsum	Endoliths
	Chwałowice	50.5651914° N, 20.6162725° E	Gypsum	Endoliths
	Wola Zagojska Górna	50.4439208° N, 20.6105317° E	Gypsum	Endoliths
Sicily (Italy)	Eraclea Minoa	37.3942910° N, 13.2892600° E	Gypsum	Endoliths
	Santa Ninfa	37.7768692° N, 12.8667633° E	Gypsum	Endoliths
	Entella	37.7694772° N, 13.1011228° E	Gypsum	Endoliths
	Ravanusa	37.3007758° N, 13.9900467° E	Gypsum	Endoliths

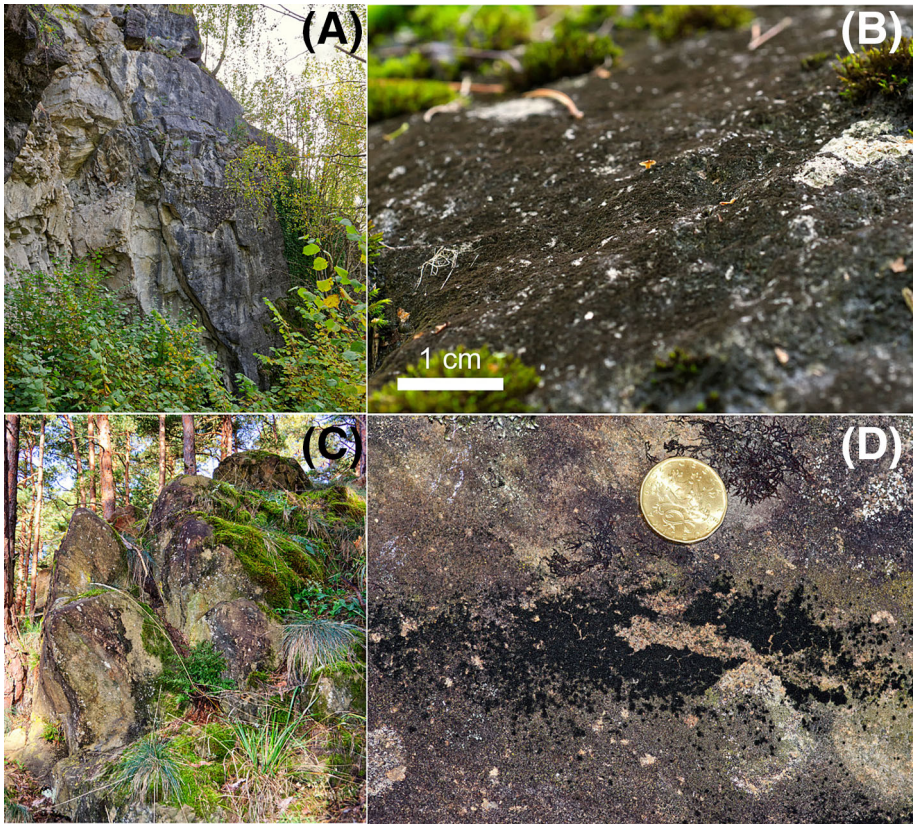

FIGURE 2 Marble and serpentinite colonised outcrops from Southern Bohemia—Opolenec marble (A) and detail of dark epilithic colonies (B), Holubov serpentinite rocks (C) and detail of black epilithic colonies (D).

2.1.4 | Chotel Czerwony

Colonised gypsum samples were collected from the ouctrop near the town Chotel Czerwony (GPS: 50.3715161° N, 20.7284994° E) (Figure 3A). Greyish-white gypsum crystals (40–60 cm in length) (Figure 3B) were found at the bottom, and in some places, these crystals were covered by dark grey coating. Uppermost black and inner green pigmented endolithic colonisation was found in honey colour narrow transparent gypsum crystals, mostly located between the greyish-white gypsum crystals.

2.1.5 | Chwałowice

Colonised crystals originate from gypsum outcrop about 100-m distance from the road from Gartatowice to

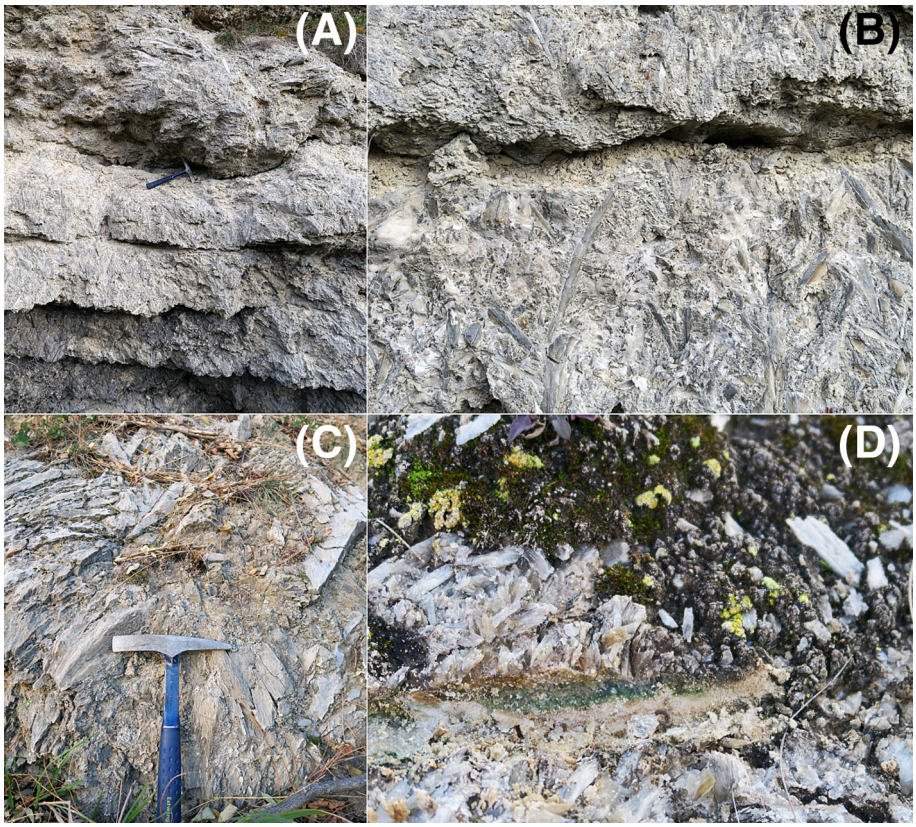

FIGURE 3 Gypsum outcrops from eastern Poland—Chotel Czerwony (A,B) and Wola Zagojska (C,D); image (D) shows green endolithic colonisations.

Chwałowice (GPS: 50.5651914° N, 20.6162725° E). Greyish flat selenitic crystals (~10 cm in length) showed no specific orientation at the outcrop, and their cleavage spaces were by black (uppermost), orange and green (inner) endoliths.

2.1.6 | Wola Zagojska

Small outcrop about 10 m from the road in Wola Zagojska Górna (GPS: 50.4439208° N, 20.6105317° E) (Figure 2C). Gypsum crystals with various orientation were colonised in their cleavage space by black (uppermost) (Figure 3D), orange and green endoliths in the inner parts of crystals.

2.1.7 | Eraclea Minoa

Endolithic colonisations were found in a gypsum-calcite outcrop about 200 m from the village Eraclea Minoa (GPS: 37.394291° N 13.289260° E). Colonised crystals were collected from the blocks of gypsum from the upper part of the outcrop. Gypsum crystals were about 10 cm long, and colonisation was located about 2–4 cm from the surface.

2.1.8 | Santa Ninfa

Flat honey-coloured selenites were collected from a gypsum outcrop near the village Santa Ninfa (GPS: 37.7768692° N, 12.8667633° E). These crystals were colonised in their cleavage spaces, frequently in the inner weathered zones.

2.1.9 | Entella

Gypsum outcrop is located near the road between Poggioreale and Borgo Roccella (GPS: 37.7694772° N, 13.1011228° E) (Figure 2A). Grey gypsum crystals formed aggregates (~5 cm in length) with underlaying fine-grained weathered matrix (Figure 4B). In this matrix, endolithic colonisations were found.

2.1.10 | Ravanusa

Gypsum outcrop is located near the road close to the town Ravanusa (GPS: 37.3007758° N, 13.9900467° E) (Figure 3C). On the surface of the outcrop, grey crystals (about 0.5–2 cm in length) were present (Figure 4D). Beneath them, weathered fine-grained matrix with endolithic colonisation occurs (about 5 cm below the surface).

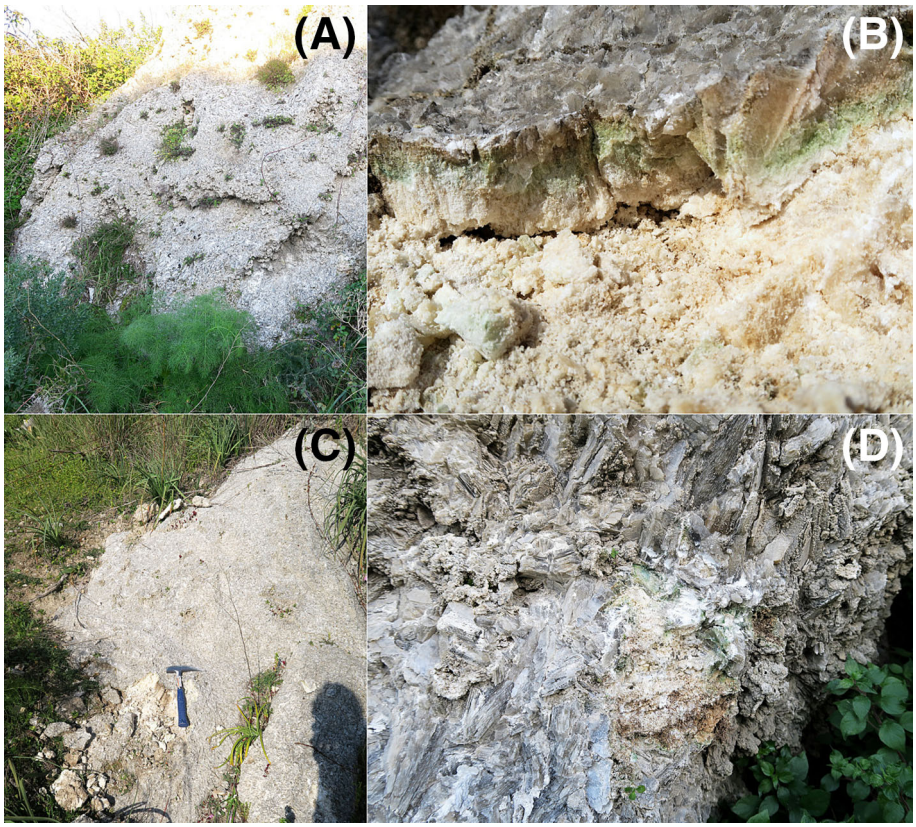

FIGURE 4 Gypsum outcrops found in Sicily—Entella (A) and Ravanusa (C) and detailed images of green endolithic colonisations at Ravanusa site (B) and Entella site (D).

2.2 | Field sampling and microscopic analysis

Samples of epilithic aerophytic microbial mats were taken by scraping from rock into sterile vials using the cap of the vial or a knife washed by distilled water, and endolithic samples were taken as small pieces of rock with visible coloured patches of microbial colonisation. The rock outcrops inside protected areas were sampled with caution to vegetation and the mineral substrate, gently removing only minor amounts (up to 2 mL) of the microbial assemblage at sites directly accessible from touristic footpaths. The samples were air-dried in the laboratory and stored at a dark and dry place for further processing.

Sampled microbial biomass was gently removed from the substrate and crushed on a microscopy slide in a drop of sterile water. Microscopic observations were accomplished using Olympus BX 51 light microscope equipped with differential interference contrast optics under 400–1000× magnification (bright field), and cyanobacteria were documented using Olympus cell Sens Standard v. 2.1 image analysis software. Cyanobacterial taxa were identified according to Komárek and Anagnostidis,[58] Komárek.[59,60] Three slides per sample were analysed to reliably identify the dominant species.

2.3 | Raman spectroscopy

Tiny amount (<1 mm^3) of each colony was sampled at random from the originally collected samples and subsequently placed on an aluminium slide and was analysed after drying. The analyses were performed at first in a screening mode, where fast analyses at many points covering the sample allowed to establish the relative occurrence of different pigments. Two Raman spectrometers were used for acquisition of the Raman spectra. The first was a Thermo Scientific DXR Raman microscope coupled with an Olympus microscope. Excitation was provided by 445-, 532- and 780-nm diode lasers. The spectra were recorded using a high-resolution grating in the range of 100–1800 cm^{-1} with a spectral resolution less than 2 cm^{-1}. Single Raman spectra were collected using 128 scans each of 2-s exposure for an improved signal-to-noise ratio. The laser spot size was approximately 2 μm in diameter when focused at the surface. Laser power used was variable for different lasers (typically 0.5–4 mW at source); however, the care was taken as to avoid any changes to the organic part of the samples and subsequent manifestations in the Raman spectra. A polystyrene standard was used for spectral wavenumber calibration. The second spectrometer was a Renishaw inVia Reflex Raman microspectrometer coupled with a Leica microscope. Excitation was provided by a 514-nm

TABLE 2 Identified dominant species of microorganisms and their typical pigments.

Lithology/site	Sample	Dominant species	Identified pigments
Marble Opolenec (CZ)	1 (3)	*Gloeocapsa alpina*, *G. novacekii*, *Scytonema* sp.	Scytonemin Scytonemin derivative
	2 (8)	*Gloeocapsa violascea*	Scytonemin Carotenoids
	3 (15)	*Scytonema* sp.	Scytonemin Carotenoids Chlorophyll
	4 (16)	*Scytonema myochrous*, *Tolypothrix elenkii*	Scytonemin Scytonemin derivative
Serpentinite Holubov (CZ)	5 (17)	*Stigonema* sp., *G. novacekii*	Scytonemin Scytonemin derivative Carotenoids Gloeocapsin
	6 (18)	*Stigonema* sp.	Scytonemin derivative Gloeocapsin Carotenoids
	7 (19)	*G. novacekii*	Scytonemin derivative Gloeocapsin Carotenoids Melanin
	8 (21)	*Hassalia byssoidea*	Scytonemin Scytonemin derivative Gloeocapsin Gloeocapsin
	9 (23)	*Hassalia byssoidea*, *Nostoc* sp.	Scytonemin Chlorophyll Carotenoids
	10 (24)	*Hassalia byssoidea*	Scytonemin Carotenoids
Gypsum Chotel Czerwony (PL)	P3	*Chroococcidiopsis*, *Gloeocapsa* sp, *Gloeocapsa violacea*, *Nostoc* sp, green algae	Scytonemin Gloeocapsin Scytonemin derivative
Gypsum Skorocice (PL)	P4	*Gloeocapsa* sp., *G. violascea*, *green algae*	Scytonemin Carotenoids
Gypsum Chwałowice (PL)	P5	*Nostoc* sp., *Chroococcidiopsis*, *Gloeocapsa* sp, *G. violascea*	Gloeocapsin Carotenoids Scytonemin
Gypsum Wola Zagojska (PL)	P9	*Gloeocapsa* sp., *G. violascea*, *Nostoc* sp.	Gloeocapsin Scytonemin Carotenoids Melanin
Gypsum Eraclea Minoa (IT)	S5	*Nostoc* sp., *Chroococcus*, *Chroococcidiopsis*, *Gloeocapsopsis pleurocapsoides*	Scytonemin Carotenoids
Gypsum Santa Ninfa (IT)	S10	*G. compacta*, *Chroococcus* sp., *G. novacekii*, *Gloeobacter violaceus*, *Gloeocapsosis rupestris*, *G. alpina*	Scytonemin Gloeocapsin Carotenoids
Gypsum Entella (IT)	S11	*Nostoc* sp., *G. compacta*, *Gloeocapsa* sp., *Gloeobacter violaceus*, *Chroococcus* sp., *G. novacekii*, *Chroococcidiopsis*, *Gloeocapsosis pleuropasoides*, *Hassalia byssoidea*	Scytonemin Carotenoids Melanin

TABLE 2 (Continued)

Lithology/site	Sample	Dominant species	Identified pigments
Gypsum Ravanusa (IT)	S13	*Gloeocapsa novacekii*, *G. compacta*, *Gloeocapsosis pleuropasoides*, *Nostoc* sp., *Symplocastrum* cf., *Chroococcidiopsis*	Scytonemin Carotenoids

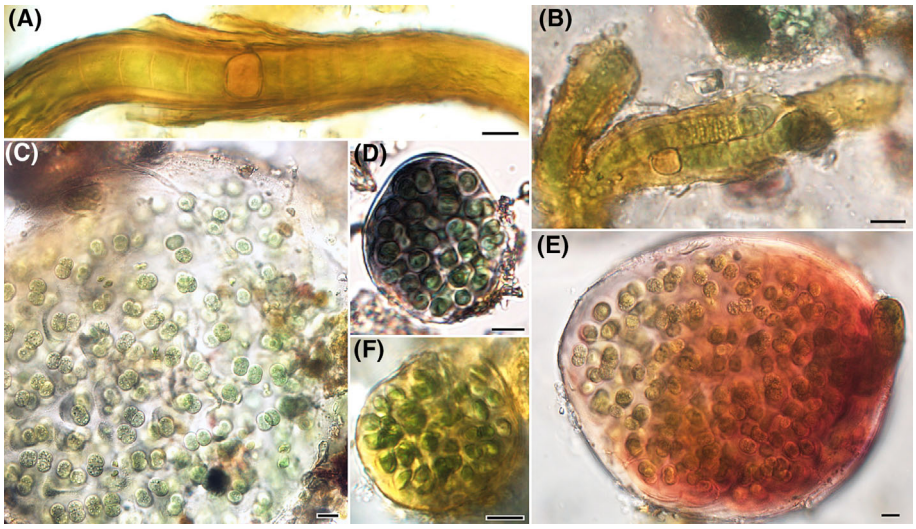

FIGURE 5 Dominant species of epilithic cyanobacteria from Opolenec, Czechia (marble) observed by light microscopy. *Scytonema myochrous* (A); *Tolypothrix elenkinii* (B); *Gloeocapsa alpine* (C); *Gloeocapsa violascea* (D); *Gloeocapsa novacekii* (E); *Gloeocapsopsis pleurocapsoides* (F). Scale bars = 10 μm.

argon laser and a 785-nm diode laser. The spectra were recorded using a high-resolution grating in the range of 100–1800 cm^{-1} with a spectral resolution less than 2 cm^{-1}. Single Raman spectra were collected using 10–30 scans each of 10-s exposure for an improved signal-to-noise ratio. Using the 50× objective, the laser spot size was approximately 2 μm in diameter when focused at the surface. Laser power used was variable for different lasers (typically 0.1–2 mW at source for the 514-nm laser and 0.3–15 mW for the 785-nm laser). Raman spectra were exported into the Galactic *.SPC format. Spectra were viewed and evaluated using GRAMS AI spectroscopy software suite (9.3, Thermo Electron Corp., Waltham, MA, USA).

3 | RESULTS

3.1 | Optical microscopy of microorganisms

3.1.1 | Microscopic observation of epilithic phototrophs from Czechia

The epilithic microbial communities at both Czech sampling sites (Opolenec and Holubov) were clearly dominated by cyanobacterial species possessing thick exopolysaccharide envelopes with content of colourful UV-screening pigments as an adaptation to periodical desiccation and direct UV radiation.[12,13] Macroscopically, the samples of epilithic colonisations consisted of thick epilithic biofilms with a structure corresponding to the dominant cyanobacterial morphotypes—filamentous biofilms were dominated by heterocytous filamentous cyanobacteria, whereas finely granular biofilms were dominated by spherical colony-forming cyanobacteria. These two prominent groups of cyanobacteria prevailed in individual samples at both sites although the species composition only partly overlapped (Table 2). The filamentous heterocytous cyanobacteria (Nostocales) with yellow-brown sheath pigments were represented by *Scytonema myochrous* (Figure 5A), *Stigonema tomentosum* (Figure 6A), *Tolypothrix elenkinii* (Figure 5B), *Hassallia byssoidea* (Figure 6B,C) and *Nostoc* sp. (Figure 6D). The colonial coccoid cyanobacteria included species with blackish violet (*Gloeocapsa violascea*—Figures 5D and 6F; *Gloeocapsa alpina*—Figure 6C), red (*Gloeocapsa novacekii*—Figures 5E and 6E; *Gloeocapsopsis dvorakii*—Figure 6G) and yellow-brown (*Gloeocapsopsis pleurocapsoides*—Figure 5F) sheath pigments.

The samples of endolithic colonisation in gypsum (Poland and Sicily) consisted of the endolithic biomass colonising the gypsum rock, either within the softer porous material or on the loose cleavage planes within gypsum. The colonisation was clearly stratified: the black

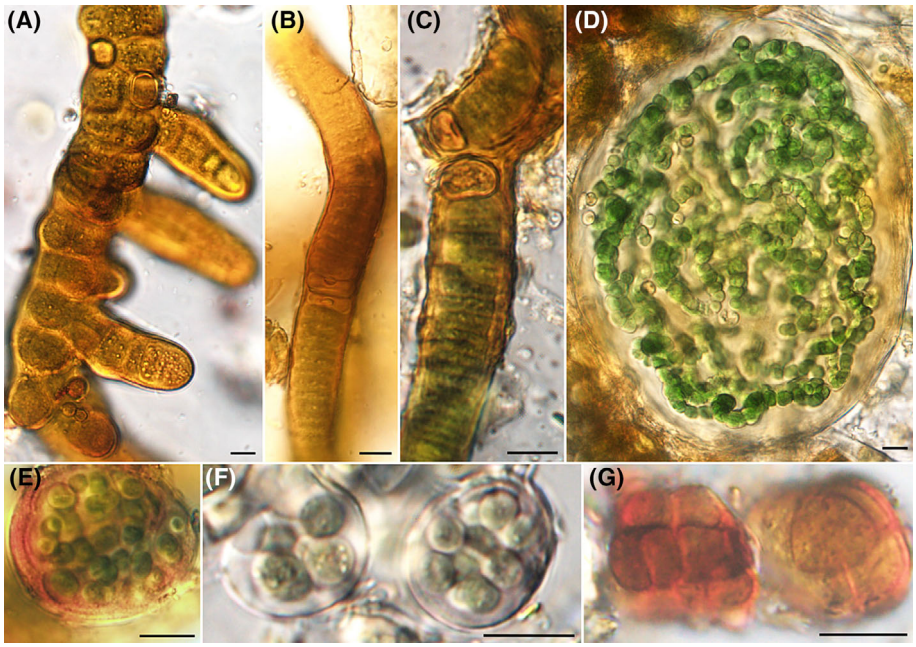

FIGURE 6 Dominant species of epilithic cyanobacteria from Holubov, Czechia (serpentinite) observed by light microscopy. *Stigonema tomentosum* (A); *Hassallia byssoidea* (B,C); *Nostoc* sp. (D); *Gloeocapsa novacekii* (E); *Gloeocapsa violascea* (F); *Gloeocapsopsis dvorakii* (G). Scale bars = 10 μm.

coloured colonisation being the closest to surface and the source of light, the red colonisation beneath and the green colonisation in the deepest parts.

3.1.2 | Microscopic observation of endolithic phototrophs from Poland

Colonised samples in Polish sites had always chasmoendolitihic character; that is, colonisation was found in the cracks and fissures of gypsum crystals. The colonisation was clearly stratified, creating at least two strata of green or black colour. In samples collected from Chotel Czerwony and Wola Zagojska sites, additional orange (middle) zones were present. The most abundant species, present in all samples, were *Nostoc* sp. (Figure 7B), *Gloeocapsa* sp. and *Gloeocapsa violascea* (Figure 7A). These species created colonies with brownish or blackish pigmented sheaths causing the overall colour of gypsum crystals. *Chroococcidiopsis* sp. was another abundant species found in samples collected from sites Chotel Czerwony and Chwałowice.

3.1.3 | Microscopic observation of endolithic phototrophs from Sicily

Similarly to colonisation in Poland, endolithic colonisations in Sicily were observed in the cracks and fissures of gypsum crystals. Compared with Polish samples, more species were found. At all sites, at least two zones of colonisations were present, usually dark/black pigmented

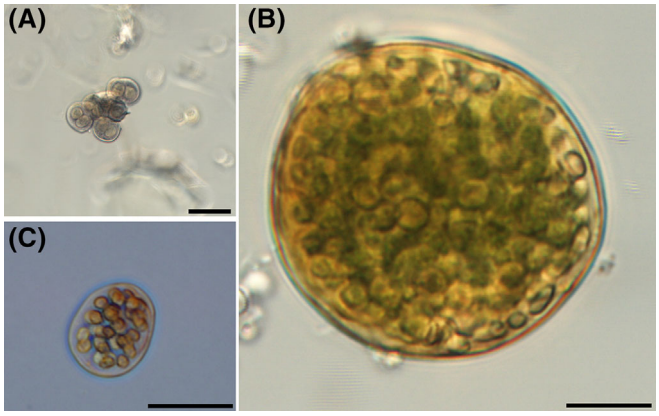

FIGURE 7 Microscopic images of the examples of the most abundant endolithic cyanobacteria, *Gloeocapsa violascea* isolated at site Wola Zagojska (A); *Nostoc* sp. from Chwałowice site (B) and *Gloeocapsa novacekii* from Entella site (C). Scale bars = 10 μm.

zone frequently colonised by sheathed colonies of *Gloeocapsa* and *Nostoc* sp. that was closer to the surface and inner green coloured areas dominated by *Chroococcidiopsis* sp. At sites Santa Ninfa, Entella and Ravanusa, orange colonisation region was present between these two zones—always above the greenish one. The orange zones contained also inorganic material, and cells were more damaged (or dead) than in the other zones of colonisation. The orange zones were colonised by various species such as *G. novacekii* (Figure 7C), *Chroococcus*, *Gloeocapsosis rupestris*, *G. compacta*, *Gloeocapsa* sp. or *Gloeobacter violaceus*.

3.2 | Raman spectroscopy

3.2.1 | Epiliths (in marbles and serpentinites, Czechia)

The samples of epilithic colonisation in marbles (Opolenec, Czechia) and in serpentinites (Holubov, Czechia) consisted of the epilithic biomass in the form of coatings. For measurements, macroscopically homogeneous blackish parts were scraped-off of the rock faces. The major pigment as well as the other minor pigments detected are listed in Table 2. For each individual and different pigment, several Raman spectra were collected with a good signal-to-noise ratio. The representative Raman spectra for each major and minor pigment detected in marbles and serpentinites are shown in Figures 8 and 9, respectively. Raman spectra of pigments presented in all the figures are listed in a descending order from the top left to bottom right roughly based on the relative abundance of the pigment. If there are more than one coloured colonisations (green and red in addition to black), the colour of the colonisation the pigments originate from is noted as well. Detailed list of the Raman bands of the detected pigments is shown in Table S1.

Because, macroscopically, the samples appeared very dark to almost black coloured (when wet), the dark brown and black biological pigments were expected to be detected.

Indeed, the major pigment detected in the samples of the epiliths both from marbles and serpentinite was scytonemin (see Table 2) with the characteristic Raman bands located at 1712 (w), 1632 (ms), 1593 (vs), 1558 (m), 1323 (mw) and 1171 cm^{-1} (ms). An additional spectroscopic signature of another dark pigment was detected in majority of the samples of endolithic colonisation. This signature while similar to the scytonemin spectrum was distinctly different and arguably belongs to one of the scytonemin derivatives. In most of the samples, the regular scytonemin was the major dark pigment; however, the scytonemin derivative was also quite commonly detected in most of the samples of epiliths, and in a few samples, it seemed to be the dominant of the species derived from the scytonemin skeleton. The detected Raman bands of this scytonemin derivative were 1650 (m), 1605 (s), 1584 (ms), 1559 (s), 1437 (ms), 1424 (ms), 1401 (mw), 1343 (mw), 1321 (m), 1258 (m) and 1185 cm^{-1} (mw). This result is further discussed later. Several other pigments were detected within the black colonisation, namely, different species of carotenoid pigments corroborated by the characteristic carotenoid signatures with the position of the ν_1 band at cca 1510, 1520 and 1525 cm^{-1}. The relatively complex carotenoid signature (Figures 8C and 9C) differs significantly from β-carotene signatures consisting of three major Raman features. Because this signature was detected at many spots with an identical spectrum (relative intensity of Raman bands), we presume that this is not a mixture of several pigments, rather a one stable complex system containing carotenoid pigment. Another pigment gloeocapsin was tentatively detected in the samples from Holubov (Figure 9D). The presence of the gloeocapsin Raman signature was however not very common in the investigated specimens of epiliths. Melanin, (eumelanin), another dark coloured UV-screening pigment, was detected on fungal hyphae structures with its characteristic signature of two broad bands located at around 1600

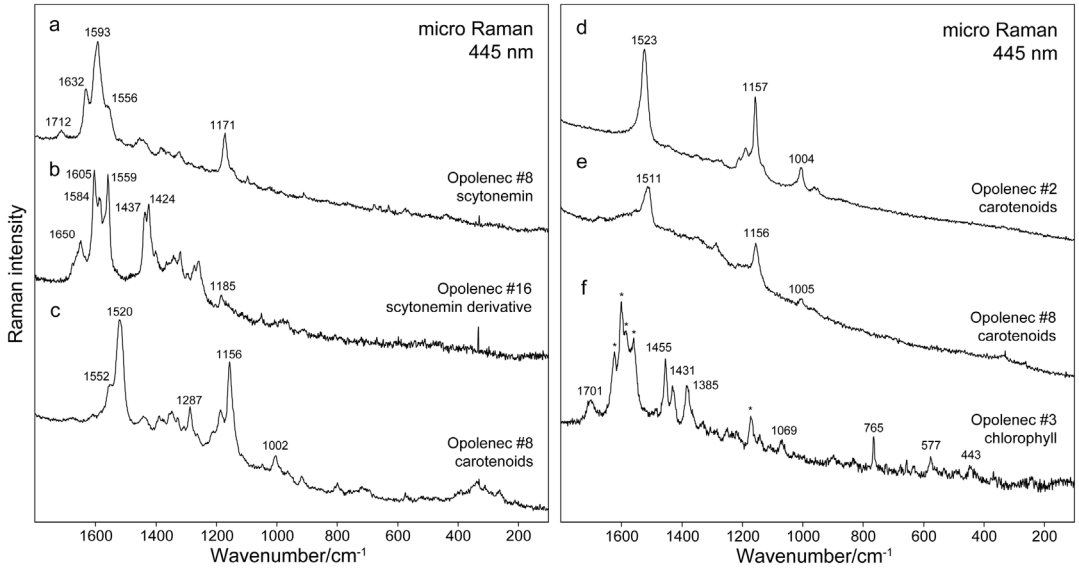

FIGURE 8 Raman spectra of pigments of epiliths in marbles at Opolenec, Czechia. An asterisk (*) denotes the scytonemin bands in Opolenec #3.

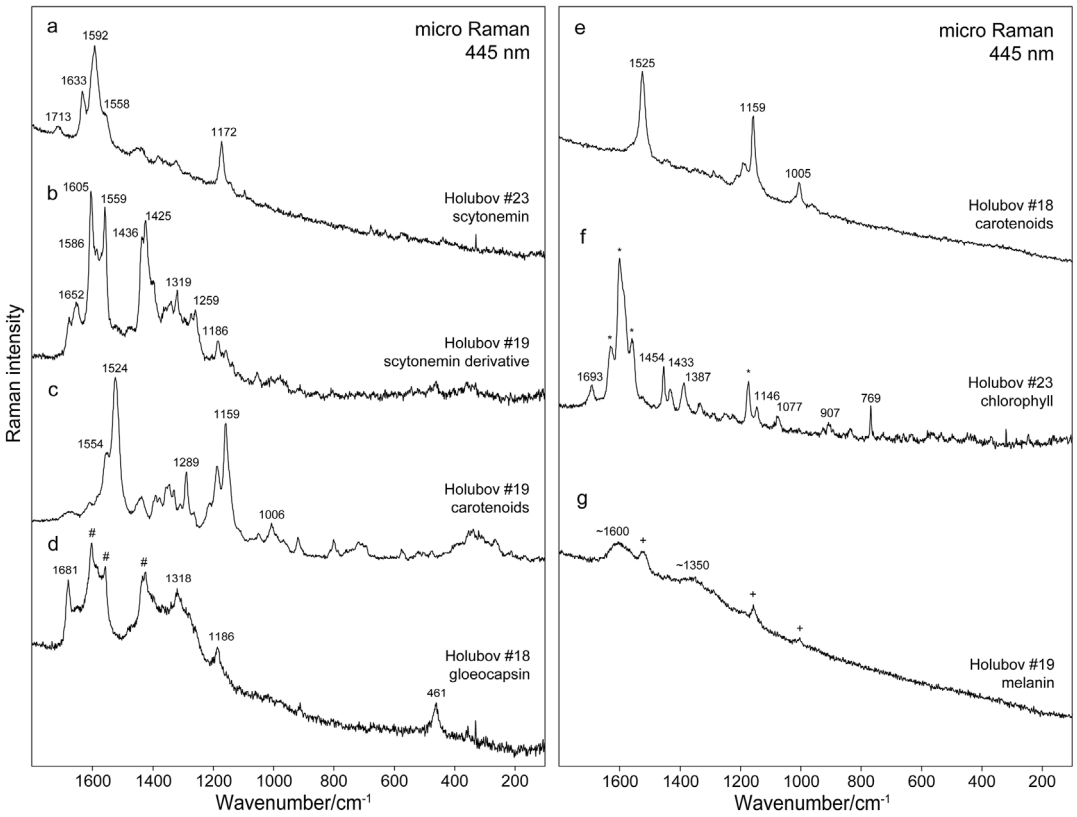

FIGURE 9 Raman spectra of pigments of epiliths in serpentinites at Holubov, Czechia. A hash (#) denotes the scytonemin derivative bands, an asterisk (*) denotes the scytonemin bands in Holubov #23 and the plus sign (+) denotes the carotenoid bands in Holubov #18 and Holubov #19.

and 1350 cm^{-1} (Figure 9G). Chlorophyll was also detected in few spots. Lastly, gloeocapsin was detected in the samples of epiliths in serpentinites (Figure 8).

3.2.2 | Endoliths (in gypsum, Poland and Sicily)

Small pieces of samples were analysed using either regular or long working distance objectives depending on the surface morphology of the sample. The use of long working distance objective allowed suitable focusing and obtaining spectra of aggregates attached inside the cavities of an uneven surface. The analyses were performed at first in a screening mode, where fast analyses at many points covering the sample allowed to establish the relative occurrence of different pigments. The major pigment as well as other minor pigments that were detected are listed in Table 2. For each individual and different pigment, several Raman spectra were collected with a good signal-to-noise ratio. The detailed summary of Raman bands of the detected pigments is listed in Table S1, and the examples of the spectra of pigments detected in gypsum endoliths from Poland and Sicily are shown in Figures 10–12.

Unlike the epiliths, the endoliths in gypsum both from Poland and Sicily showed distinct stratification into black, red and green zones of colonisation. In the samples from Poland, the most frequently occurring pigments were scytonemin: 1711 (mw), 1633 (m), 1600 (s), 1558 (m) and 1174 cm^{-1} (ms); and gloeocapsin: 1672 (ms), 1573 (m), 1328 (ms, sh), 1288 (ms), 467 (m). The pigment gloeocapsin was significantly more abundant in the gypsum samples from Poland than in either marbles and serpentinites from the Czechia or samples of gypsum from Sicily. In the samples of gypsum endoliths from Poland (Chotel Czerwony locality), we again found the scytonemin derivative mentioned previously, as corroborated by the bands at 1648 (m), 1603 (s), 1586 (ms), 1559 (s), 1437 (ms), 1425 (ms), 1320 (m) and 1259 cm^{-1} (m). Melanin pigment was found in the samples of gypsum endoliths from Poland, as evidenced in the broad features at 1615 and 1360 cm^{-1} (see Figures 10D and 11D). Carotenoids were detected in the zones of all colours. In the black colour colonisation, the position of the carotenoid ν_1 Raman bands was typically 1512–13 cm^{-1}, carotenoids within the red zone showed strong signal with the position of the ν_1 band at 1513–14 cm^{-1} and the carotenoids in the green zone the ν_1 band was located at 1520 cm^{-1}. The

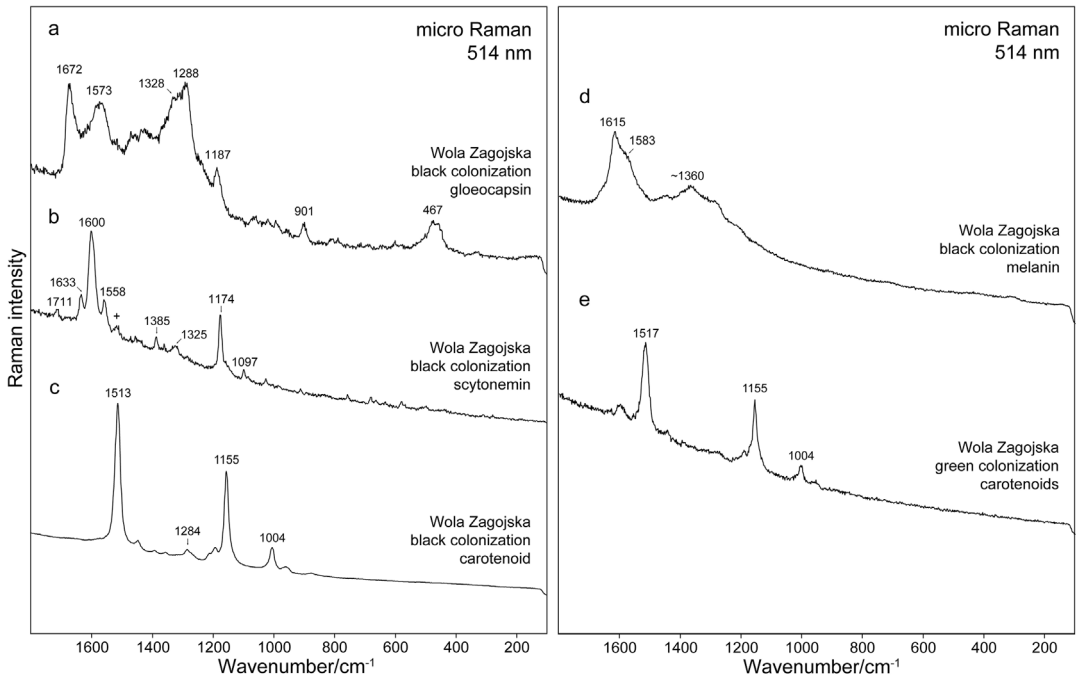

FIGURE 10 Raman spectra of pigments of endoliths in gypsum from Wola Zagojska, Poland. The plus sign (+) denotes the carotenoid band.

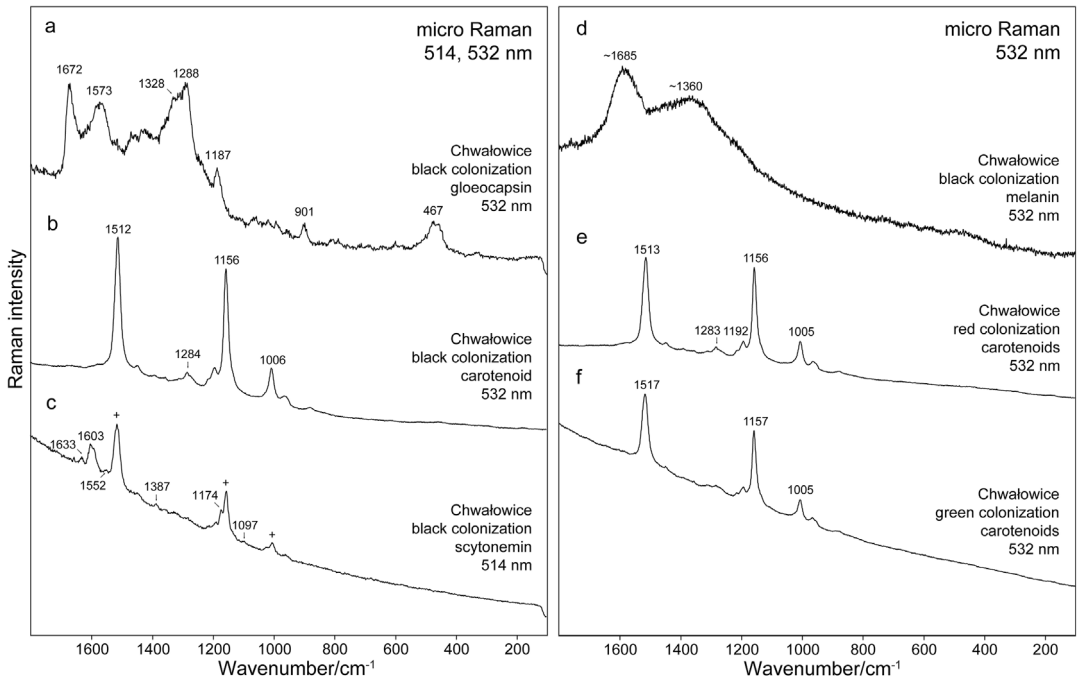

FIGURE 11 Raman spectra of pigments of endoliths in gypsum from Chwałowice, Poland. The plus sign (+) denotes the carotenoid bands in Chwalowice (c).

complex carotenoid signature (see Figures 8C and 9C) was detected only in the samples from Sicily (see bottom spectra in Figure 12Ac and Bd). Using a 785-nm excitation, chlorophyll and phycobilliproteins were detected in the green zone (see Table S1).

4 | DISCUSSION

Interesting cyanobacterial colonisations were described from hot environments in tropical areas from Latin America where they develop on rocky (frequently granitic)

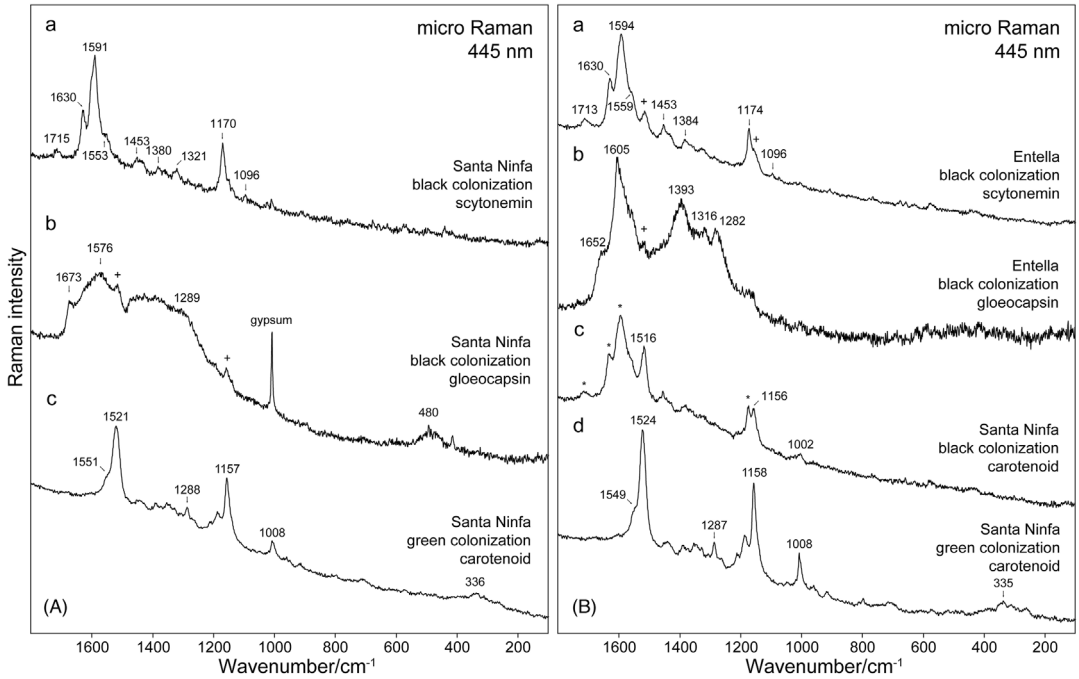

FIGURE 12 Raman spectra of pigments of endoliths in gypsum from Santa Ninfa, Sicily (A) and from Entella, Sicily (B). A plus sign (+) denotes carotenoid bands in Santa Ninfa (b) and Entella (a,b) and the asterisk (*) denotes the scytonemin bands in Santa Ninfa (c).

inselbergs. Bultel-Poncé et al.[61] have described the presence of photoprotective pigments in cyanobacterial colonies of *Scytonema* sp. growing on granite at Mitaraka Inselberg (French Guyana). Pigments detected in extracts from these epiliths include scytonemin, dimethoxyscytonemin, tetramethoxyscytonemin and scytonin. The molecular structures of all three derivatives have been determined by nuclear magnetic resonance (NMR) and infrared (IR) spectroscopy[61] and have already been discussed with respect to their theoretical Raman spectra predicted on the basis of *ab initio* Hartree-Fock (HF) and Density Functional Theory (DFT) calculations.[62] Some of the derivatives have not yet been characterised experimentally using Raman spectroscopy. Recently, we succeeded to record Raman spectra of a derivative[63] with Raman features very similar to those of previously theoretically predicted scytonin.[61] More detailed investigation of the distribution of scytonin and other scytonemin derivatives from gypsum endoliths is currently in preparation.

Scarce investigations reported epilithic colonisations and interaction with outcropping bedrock using Raman spectroscopy. These focus mostly on detecting photosynthetic or UV-protective pigments. Some epiliths and endoliths from cold Antarctic areas, their colonists (lichens, cyanobacteria) and Raman spectra of their pigments were reported by Jehlička et al.[47] Common pigments detected from these environments included β-carotene, chlorophyll, scytonemin, rhisocarpic acid and parietin. Raman spectra of native epiliths from reddish biofilm located on the sandstone from the Northside of La Galea Fortress (Getxo, North of Spain) were collected by Morillas et al.[64] Here, authors report β-carotene, scytonemin and haloarchaeal C50 carotenoid connected to the colonising alga *Trentepohlia*. The biofilms from the granitic Sacred Rock from the Machu Picchu Inca sanctuary (Cusco Region, Peru) contain rich biocolonisations. Raman spectra of studied epiliths showed the presence of carotenoids of different lengths of the conjugated chain, chlorophyll and scytonemin.[65] Desert varnish is another geological material from where epilithic colonisation was described in hot and dry desertic zones. Dark desert varnish specimens from Colorado contain for instance besides β-carotene also scytonemin, as shown by the diagnostic Raman bands.[66] Parts of natural geological outcrops of limestone colonised at Pont de Bonne, Hoyoux Valley, Modave, Belgium are covered by dark cyanobacterial colonies. Here, an important Raman spectroscopic study showed the presence of scytonemin and also gloeocapsin, an enigmatic pigment from cyanobacterial epilithic sheats.[29,30]

In the present report, two sites with different lithology of the epilithic colonisation were investigated, both from South Bohemia—serpentinite and marble. Epilithic or endolithic colonisations of similar weathered peridotitic rocks—serpentinites—were described scarcely.

Sigal[67] described interesting associations of lichens on peridotites and serpentinites in the frame of few sites in California. Lichens growing on ultramafic rocks of different types including serpentinite at New Idria (California) area were described and catalogised by Rajakanura et al.[68] The specific cyanobacterial microflora of serpentinite rocks was previously studied in Holubovské hadce nature reserve (one of our sampling localities) by Hauer[69] and Mohelenská hadcová step nature reserve by Nováček[70] and Hauer[71] The species composition in our samples from Holubov was in agreement with the data by Hauer,[69] documenting long-term dominance of *H. byssoidea*, *G. dvorakii*, *G. violascea* and *Stigonema* spp.

Marble and its epilithic colonisations are described more commonly. A comparison of occurrences and processes in carbonate rocks colonized by lithobionths – lichens and endolithic cyanobacteria was given by Hoppert et al.[72] Macedo et al.[19] reviewed the reports of the occurrences of algal and cyanobacterial deterioration of monuments in the Mediterranean area. They show that about 37 genera of cyanobacteria and 48 genera of chlorophyta are encountered in such colonisations mostly on limestone, marble and travertines. The composition of epilithic cyanobacterial communities growing on non-aquatic limestone substrates was thoroughly reviewed in Hauer et al.[13] Our sampling site for limestone epiliths, Opolenec, was previously briefly investigated by Hauer.[69]

Endolithic mode of colonisation of rocks by cyanobacteria and algae seems to be reported and investigated more commonly. Some rocks—sandstones, gypsum, halite, dolomites or limestones—are colonised more commonly, and reports on these interactions show different examples.[2,38,73,74] Raman spectroscopic investigations of such stony colonisations were reported since the end of 20th century. Such spectroscopic studies of endolithic colonisations focused, interestingly, on areas of stressed environments. First excellent reports on common photosynthetic pigments and their Raman spectra originate from Antarctic area.[40,74] Contrary to these environments, Wierzchos et al.[38] reported the presence of scytonemin in the cyanobacteria from hypoendolithic habitat in gypsum in Atacama. Previously, Vítek et al.[4] did not report scytonemin using Raman spectroscopy of phototropic communities in gypsum. However, Raman spectra showed common presence of scytonemin within the cyanobacterial colonisation in halite crusts from the same desert area.[36,53]

Examples of rocky colonisations documented in this report fall clearly in the group of endoliths of mild climatic conditions. Mediterranean area as well as major parts of Europe belongs to areas of mild climatic conditions. Summer temperatures do not exceed 35°C. Winter frosts can be significant in mountain areas but generally prolonged low temperature periods are not common in the Mediterranean or European lowlands. Annual rainfall in the Mediterranean area does not exceed 250 mm. Higher rainfall is common in mountainous areas. The Raman spectroscopic data collected on a series of gypsum endoliths from Sicily confirm the almost ubiquitous presence of scytonemin in dark parts of samples investigated.[5,56] Studies of gypsum endolithic outcrops in Eastern Poland confirm the same common presence of this protective pigment.[56] The distribution of prevalent cyanobacterial UV-protective pigments in our study generally followed the distribution of dominant species as documented by light microscopy (Table 2). In macroscopically dark-brown and blackish epilithic samples from marble and serpentinite substrates, dominated by filamentous (*Scytonema*, *Stigonema*, *Tolypothrix*, *Hassallia*) and coccoid (*G. pleurocapsoides*) cyanobacteria with yellow-brown sheath pigmentation, scytonemin (or its derivative) was unambigously detected as the most abundant pigment. Scytonemin was further recorded in endolithic samples, mostly those containing *Nostoc* sp. colonies, again with yellow-brown pigmentation. These data support the previously demonstrated wide phylogenetic span of scytonemin biosynthesis across multiple cyanobacterial orders.[21]

Another special pigment reported in the studied samples is a derivative of scytonemin from cyanobacterial colonies in marble and serpentinite (Czechia) and scarcely also from gypsum from Poland. It was however challenging to link the putative scytonemin derivative to any specific cyanobacterial species. The compound, as identified by Raman spectroscopy, occurred in samples dominated by *S. tomentosum* (Figure 6A) and samples with *S. myochrous* (Figure 5A), *T. elenkinii* (Figure 5B) and *Nostoc* sp. but lacking *Stigonema*. Therefore, it seems that the compound may serve as a more widespread UV-protective scytonemin analogue in a variety of nostocalean cyanobacteria. Obtained spectra (Figures 7 and 8) and diagnostic features resemble those predicted for scytonin by Varnali and Edwards.[62] Scytonin differs structurally from the dimethoxy- and tetramethoxy-substituted derivatives of scytonemin in that the scytonemin symmetrical dimeric structure is completely transformed. Raman signatures obtained here (samples 3 and 16 from Opolenec, 17–19 from Holubov, P3) match well with the published DFT calculations of scytonemin derivative scytonin. Another study further deepens the knowledge on the possibility of the presence of this scytonemin derivative in endoliths (epiliths). (Edwards et al.).[63]

Interestingly, the Raman signatures of another enigmatic UV-absorbing pigment gleocapsin were recorded not only in samples with high content of blackish-violet

Gloeocapsa (especially *G. violascea*—Figures 5D and 6F) but also in samples clearly dominated by the red *G. dvorakii* (Figure 6G) in serpentinite samples. This is an unexpected finding, difficult to explain in the absence of the knowledge on the precise chemical structure of gloeocapsin or its putative derivatives.[30,56] In the traditional concept, gloeocapsin should appear violet in the pH range of calcite and serpentinite substrates,[29,75] as documented by *G. violascea* occurring in the same samples. Diagnostic Raman features of this pigment present in the spectra of gypsum endoliths from Poland were found at 1674, 1669, 1574, 1287 and 1276, 902 and 463–465 cm^{-1}. Results of a detailed study on the characteristics and distribution of gloeocapsin in European gypsum endoliths using Raman spectroscopy will be presented in a forthcoming study.

5 | CONCLUSIONS

The presence of the UV-protective pigment scytonemin was documented using conventional Raman spectrometry in marble and serpentinite epiliths and gypsum endoliths at several sites from mild environmental conditions from Central Europe and Sicily. Based on our results, scytonemin is likely produced by a wide range of cyanobacterial epilithic and endolithic representatives from the orders Nostocales (*Scytonema*, *Stigonema*, *Hassallia*, *Tolypothrix*, *Nostoc*) and Chroococcidiopsidales (*Gloeocapsopsis*), growing on a variety of aerial rocky substrates. Melanin and gloeocapsin are other pigments detected additionally in few samples of rock-inhabiting biofilms. General similarities with gypsum endoliths and their Raman spectra showing the presence of scytonemin, carotenoids, gloeocapsin and melanin are shown and discussed. Interestingly, gloeocapsin was tentatively detected also in *Gloeocapsopsis dvorakii*, a coccal cyanobacterium with red pigmentation on basic substrate, and it reportedly has blackish-violet colour in co-occurring species of *Gloeocapsa*. Raman spectra of a derivative of scytonemin, tentatively supposed to be close to scytonin, were repeatedly recorded as well in samples dominated by multiple species of heterocytous filamentous cyanobacteria. A forthcoming study will further develop Raman spectroscopic search of scytonemin derivatives in cyanobacteria. Then, a comparison of Raman spectroscopic results from endolithic and epilithic cyanobacterial colonisations with existing theoretical data obtained from calculations of scytonemin derivatives as already published will be an option to confirm the hypothesis.

ACKNOWLEDGEMENTS

This project was supported by the Czech Science Foundation, Project 21-03322S and Center for Geosphere Dynamics (UNCE/SCI/006). We would like to thank Filip Košek for the assistance including taking the photographic materials and preparation of several figures. We greatly appreciate the access to the DXR Raman microscope for which we thank Ivan Němec from the Department of Inorganic Chemistry of the Faculty of Science, Charles University.

ORCID

Jan Jehlička https://orcid.org/0000-0002-4294-876X
Adam Culka https://orcid.org/0000-0002-1861-070X
Kateřina Němečková https://orcid.org/0000-0002-7793-5766
Jan Mareš https://orcid.org/0000-0002-5745-7023

REFERENCES

[1] J. J. Walker, N. R. Pace, *Annu. Rev. Microbiol.* **2007**, *61*, 331.
[2] J. Wierzchos, A. de los Ríos, C. Ascaso, *Int. Microbiol.* **2012**, *15*, 172.
[3] W. Sajjad, N. Ilahi, S. C. Kang, A. Bahadur, S. Zada, A. Iqbal, *Int. Biodeter. Biodegr.* **2022**, *169*, 105387.
[4] P. Vítek, B. Camara-Gallego, H. G. M. Edwards, J. Jehlička, C. Ascaso, J. Wierzchos, *Geomicrobiol. J.* **2013**, *30*, 1.
[5] J. Jehlička, A. Culka, J. Mareš, *J. Raman Spectrosc.* **2019**, *51*, 9.
[6] C. A. Crispim, P. M. Gaylarde, C. C. Gaylarde, *Curr. Microbiol.* **2003**, *46*, 79.
[7] T. Horath, R. Bachofen, *Microb. Ecol.* **2009**, *58*, 290.
[8] A. de los Ríos, J. Wierzchos, L. G. Sancho, T. A. Green, C. Ascaso, *Lichenologist* **2005**, *37*, 1.
[9] B. P. de Oliveira, J. M. de la Rosa, A. Z. Miller, C. Saiz-Jimenez, A. Gomez-Bolea, M. A. S. Braga, A. Dionisio, *Environ. Earth Sci.* **2011**, *63*, 1677.
[10] J. Wierzchos, M. C. Casero, O. Artieda, C. Ascaso, *Curr. Opin. Microbiol.* **2018**, *43*, 124.
[11] S. Golubic, E. I. Friedmann, J. Schneider, *J. Sediment. Res.* **1981**, *51*, 475.
[12] A. A. Gorbushina, *Environ. Microbiol.* **2007**, *9*, 1613.
[13] T. Hauer, R. Mühlsteinová, M. Bohunická, J. Kaštovský, J. Mareš, *Biodivers. Conserv.* **2015**, *24*, 759.
[14] O. Huber, Vegetation, in *Flora of the Venezuelan Guayana*, (Eds: J. A. Steyermark, P. E. Berry, B. K. Holst) Vol. 1, Timber Press, Portland, OR **1995** 97.
[15] B. Budel, *Eur. J. Phycol.* **1999**, *34*, 361.
[16] B. Budel, D. C. J. Wessels, *Algol. Stud. Archiv Hydrobiol. Suppl.* **1991**, *64*, 385.
[17] O. Jaag, *Beiträge Zur Kryptogamenflora der Schweiz* **1945**, *9*, 1.
[18] M. F. Fiore, C. L. Sant Anna, M. T. P. Azevedo, J. Komárek, J. Kaštovský, J. Sulek, A. S. Lorenzi, *J. Phycol.* **2007**, *43*, 789.
[19] M. F. Macedo, A. Z. Miller, A. Dionisio, C. Saiz-Jimenez, *Microbiology* **2009**, *155*, 3476.
[20] N. Keshari, S. P. Adhikary, *Int. Biodeter. Biodegr.* **2014**, *90*, 45.

[21] P. M. D'Agostino, J. N. Woodhouse, H. T. Liew, L. Sehnal, R. Pickford, H. L. Wong, B. P. Burns, B. A. Neilan, *Environ. Microbiol.* **2019**, *21*, 702.
[22] A. Oren, Characterization of pigments of prokaryotes and their use in taxonomy and classification, in *Taxonomy of prokaryotes - methods in microbiology*, (Eds: F. A. Rainey, A. Oren) Vol. 38, Elsevier/Academic Press, Amsterdam **2011**, pp. 262–283.
[23] D. M. Pereira, P. Valentao, P. B. Andrade, *Dyes and Pigments* **2014**, *111*, 124.
[24] A. Oren, Pigments of halophilic microorganisms, in *Halophilic microorganisms and their environments: Cellular origin, life in extreme habitats and astrobiology*, The Netherlands, Springer, Dordrecht **2002**, pp. 173–206.
[25] C. Engelhard, I. Chizhov, F. Siebert, M. Engelhard, *Chem. Rev.* **2018**, *118*, 10629.
[26] H. G. M. Edwards, I. B. Hutchinson, R. Ingley, J. Jehlička, *Phil. Trans. Roy. Soc A* **2014**, *372*, 20140193.
[27] E. W. Schwierteman, C. S. Cockell, V. S. Meadows, *Astrobiology* **2015**, *15*, 341.
[28] M. Dogs, S. Voget, H. Teshima, J. Petersen, K. Davenport, H. Dalingault, A. Chen, A. Pati, N. Ivanova, L. A. Goodwin, P. Chain, J. C. Detter, S. Standfest, M. Rohde, S. Gronow, N. C. Kyrpides, T. Woyke, M. Simon, H.-P. Klenk, M. Goker, T. Brinkhoff, *Stand Genomic Sci.* **2013**, *9*, 334.
[29] J. Y. Storme, S. Golubic, A. Wilmotte, J. Kleinteich, D. Velázquez, E. J. Javaux, *Astrobiology* **2015**, *15*, 843.
[30] Y. J. Lara, A. McCann, C. Malherbe, C. Francois, C. F. Demoulin, M. C. Sforna, G. Eppe, E. De Pauw, A. Wilmotte, P. Jacques, E. J. Javaux, *Astrobiology* **2022**, *22*, 735.
[31] H.-P. Grossart, M. Thorwest, I. Plitzko, T. Brinkhoff, M. Simon, A. Zeeck, *Internat. J. Microbiol.* **2009**, *2009*, 701735.
[32] R. P. Sinha, D.-P. Hader, *Plant Sci.* **2008**, *174*, 278.
[33] Q. Gao, F. Garcia-Pichel, *Nat. Rev. Microbiol.* **2011**, *9*, 791.
[34] R. P. Rastogi, D. Madamwar, A. Incharoensakdi, *J. Appl. Microbiol.* **2015**, *119*, 753.
[35] R. P. Rastogi, A. Incharoensakdi, *FEMS Microbiol. Ecol.* **2014**, *87*, 244.
[36] P. Vítek, J. Jehlička, H. G. M. Edwards, I. Hutchinson, C. Ascaso, J. Wierzchos, *Phil. Trans. Roy. Soc. A* **2014**, *372*, 20140196.
[37] P. Vítek, J. Jehlička, C. Ascaso, V. Mašek, B. Gomez-Silva, H. Olivares, J. Wierzchos, *FEMS Microbiol. Ecol.* **2014**, *90*, 351.
[38] J. Wierzchos, J. DiRuggiero, P. Vítek, O. Artieda, V. Souza-Egipsy, P. Škaloud, M. Tisza, A. F. Davila, C. Vilchez, I. Garbayo, C. Ascaso, *Front. Microbiol.* **2015**, *6*, 934.
[39] M. C. Casero, C. Ascaso, A. Quesada, H. Mazur-Marzec, J. Wierzchos, *Front. Microbiol.* **2021**, *11*, 614785.
[40] H. G. Edwards, C. D. Moody, E. M. Newton, S. E. Villar, M. J. Russell, *Icarus* **2005**, *174*, 560.
[41] S. E. Jorge-Villar, H. G. M. Edwards, L. G. Benning, *Anal. Bioanal. Chem.* **2011**, *401*, 2927.
[42] P. Proteau, W. Gerwick, F. Garcia-Pichel, R. Castenholz, *Experientia* **1993**, *49*, 825.
[43] F. Garcia-Pichel, R. Castenholz, *J. Phycol.* **1991**, *27*, 395.
[44] J. C. Merlin, *Pure Appl. Chem.* **1985**, *57*, 785.
[45] H. Hayashi, H. Hamaguchi, M. Tasumi, *Chem. Lett.* **1983**, *12*, 1857.
[46] J. C. Merlin, *J. Raman Spectrosc.* **1987**, *18*, 519.
[47] J. Jehlička, H. G. M. Edwards, A. Oren, *Appl. Environ. Microbiol.* **2014**, *80*, 3286e3295.
[48] L. F. Maia, V. F. De Oliveira, H. G. M. Edwards, L. F. C. De Oliveira, *ChemPhysChem* **2021**, *22*, 231e249.
[49] P. Vítek, J. Jehlička, H. G. M. Edwards, I. Hutchinson, C. Ascaso, J. Wierzchos, *Astrobiology* **2012**, *12*, 1095.
[50] K. Němečková, J. Jehlička, A. Culka, *J. Raman Spectrosc.* **2022**, *53*, 630.
[51] H. G. M. Edwards, N. C. Russell, D. D. Wynn-Williams, *J. Raman Spectrosc.* **1997**, *28*, 685.
[52] H. G. M. Edwards, E. M. Newton, D. D. Wynn-Williams, R. I. Lewis-Smith, *Spectrochim. Acta, Part A* **2003**, *59*, 2301.
[53] P. Vítek, H. G. M. Edwards, J. Jehlička, C. Ascaso, A. de los Ríos, S. Valea, S. E. Jorge Villar, A. F. Davila, J. Wierzchos, *Phil. Trans. Roy. Soc. A* **2010**, *368*, 3205.
[54] G. H. Wang, Z. J. Hao, Z. B. Huang, L. Z. Chen, X. Y. Li, C. X. Hu, Y. D. Liu, *Astrobiology* **2010**, *10*, 783.
[55] H. G. M. Edwards, F. Garcia-Pichel, E. M. Newton, D. D. Wynn-Williams, *Spectrochim. Acta, Part A* **1999**, *56*, 193.
[56] K. Němečková, A. Culka, I. Němec, H. G. M. Edwards, J. Mareš, J. Jehlička, *J. Raman Spectrosc.* **2021**, *52*, 2633.
[57] K. Němečková, J. Jehlička, A. Culka, *J. Raman Spectrosc.* **2020**, *51*, 1127.
[58] J. Komárek, K. Anagnostidis, in *Cyanoprokaryota. 1. Teil: Chroococcales, Süßwasserflora von Mitteleuropa 19/1*, (Eds: H. Ettl, G. Gärtner, H. Hyenig, D. Mollenhauer), Spektrum, Heidelberg **1999**, pp. 1–548.
[59] J. Komárek, in *Cyanoprokaryota. Teil 2: Oscillatoriales, Süßwasserflora von Mitteleuropa 19/2*, (Eds: B. Büdel, L. K. Gärtner, M. Schagerl), Elsevier, München **2005**, pp. 1–759.
[60] J. Komárek, in *Cyanoprokaryota. Teil 3: Heterocystous Genera, Süßwasserflora von Mitteleuropa 19/3*, (Eds: B. Büdel, G. Gärtner, L. Krienitz, M. Schager), Springer, Berlin **2013**, pp. 1–1130.
[61] V. Bultel-Poncé, F. Félix-Théodose, C. Sarthou, J.-F. Ponge, B. Bodo, *J. Nat. Prod.* **2004**, *67*, 678.
[62] T. Varnali, H. G. M. Edwards, *J. Mol. Model.* **2014**, *20*, 2157.
[63] H. G. M. Edwards, J. Jehlička, K. Němečková, A. Culka, *Spectrochim. Acta, Part A* **2023**, *292*, 122406.
[64] H. Morillas, M. Maguregui, I. Marcaida, J. Trebolazabala, I. Salcedo, J. M. Madariaga, *Microchem. J.* **2015**, *121*, 48.
[65] H. Morillas, M. Maguregui, E. Gallego-Cartagena, G. Huallparimachi, I. Marcaida, I. Salcedo, L. F. O. Silva, F. Astete, *Sci. Total Environ.* **2019**, *654*, 1379.
[66] H. G. M. Edwards, C. A. Moody, S. E. J. Villar, R. Mancinelli, *J. Raman Spectrosc.* **2004**, *35*, 475.
[67] L. L. Sigal, *Mycotaxon* **1989**, *34*, 221.
[68] N. Rajakaruna, K. Knudsen, A. M. Fryday, R. E. O'Dell, N. Pope, F. C. Olday, S. Woolhouse, *Lichenologist* **2012**, *44*, 695.
[69] T. Hauer, *Nova Hedwigia* **2007**, *85*, 379.
[70] F. Nováček, Epilithické sinice serpentinů mohelenských [Epilithic cyanobacteria of serpentines near Mohelno] Pars I.: Chroococcales, in *Mohelno*, (Ed: J. Podpěra), Svaz pro ochranu

přírody a domoviny v zemi Moravskoslezské, Brno **1934**, pp. 1-178.
[71] T. Hauer, *Fottea* **2008**, *8*, 129.
[72] M. Hoppert, C. Flies, W. Pohl, J. Schneider, B. Gunzl, *Environ. Geol.* **2004**, *46*, 421.
[73] S. D. J. Archer, A. de los Ríos, K. C. Lee, T. S. Niederberger, S. C. Cary, K. J. Coyne, S. Douglas, D. C. Lacap-Bugler, S. B. Pointing, *Polar Geol.* **2017**, *40*, 997.
[74] D. D. Wynn-Williams, H. G. M. Edwards, F. Garcia-Pichel, *Eur. J. Phycol.* **1999**, *34*, 381.
[75] O. Jaag, *Verhandl. Schweiz. Naturforsch. Gesell.* **1940**, *120*, 157.

SUPPORTING INFORMATION

Additional supporting information can be found online in the Supporting Information section at the end of this article.

How to cite this article: J. Jehlička, A. Culka, K. Němečková, J. Mareš, *J Raman Spectrosc* **2023**, *54*(11), 1280. https://doi.org/10.1002/jrs.6514